Chemical Physics 573 (2023) 112004

Contents lists available at ScienceDirect

Chemical Physics

journal homepage: www.elsevier.com/locate/chemphys

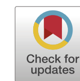

Dipole behavior in thin film heterostructure composed of Er-doped SnO_2 and GaAs: Influence of polarization bias, temperature and stray light

Fabricio T. Russo, Diego H.O. Machado, Luis V.A. Scalvi *

UNESP, São Paulo State University, Lab. of Electro-Optical Experiments on Materials Dept. of Physics, FC and Graduate Program in Materials Science and Technology (POSMAT), Bauru, SP, Brazil

ARTICLE INFO

Keywords:
TSDC
Gallium arsenide
Tin dioxide
Defects
Heterostructure
Electrical dipoles

ABSTRACT

The heterostructure system GaAs/SnO_2 is built by resistive evaporation of Er-doped SnO_2 powder on the top of GaAs semi-insulating substrate. The SnO_2 powder comes from the drying of SnO_2 sol-gel solution. The possible formation of dipoles in this heterostructure is investigated by the thermally stimulated depolarization current (TSDC) technique, and the possibilities for dipole formation are explored, such as the EL2 defect in the GaAs side, oxygen vacancies and Er ions in the SnO_2 layer. The dipole relaxation activation energies are found in the range 0.2 eV to 0.3 eV, in good agreement with the ionization energies of these defects. The main TSDC bands: 213 meV with peak of −298 pA, for positive bias, and 218 meV with peak of 128 pA for negative bias, are modified by stray (room) light, which may correspond to the second ionization level of oxygen vacancies in SnO_2, which are excited by the room lights and do not return to the original orientation.

1. Introduction

Deposition of SnO_2 on top of GaAs, forming a heterostructure, has provided some very interesting phenomena such as the interfacial conduction, similar to a two-dimensional electron gas (2DEG) [1,2] or the rare-earth emission on the photoluminescence (PL) spectra, not available when the SnO_2 layer is deposited on top of glass substrates [3,4]. The emission and/or its absence in SnO_2 thin films deposited on different sort of substrates may be investigated using Synchrotron radiation experiments, and the differences on the XANES (X-ray absorption near edge structure) related to the matrix disorder, are found as responsible [5] for the differences in the emission spectra from Eu emission, since films deposited on glass substrate do not present Eu PL transitions until the annealing temperatureis rather high.The relative intensity of the Eu or Er transitions when the ion is substitutional to Sn^{4+} or located at the grain boundary is dependent on the annealing temperature, which can be associated to the increase in the concentration of symmetric sites with temperature, which also affects the crystallite growth. Concerning Er-doping in SnO_2, one of the compounds investigated in the present work, the annealing temperature influences the Er ion location, that reflects on the PL related to $^2H_{11/2}\rightarrow{}^4I_{15/2}$ and $^4S_{3/2}\rightarrow{}^4I_{15/2}$ Er^{3+} transitions [6].

Moreover, a broad PL band is observed in this sort of samples, which can be also originated from de disorder in the structure, but often is associated with electron transfer from oxygen vacancies and the acceptor level formed by the rare-earth ions [3,7]. In either way, there are a lot of possibilities for the existence of charged defects inside the SnO_2 sample, which suggests the possible formation of dipoles.

Although emission from SnO_2 rare-earth doped powder samples is widely known and published, this emission from the heterostructure GaAs/SnO_2 in the form of thin films is highly desirable, since it makes possible the integration of this assembly in optoelectronic systems.

Dipoles may be investigated by the thermally stimulated depolarization current (TSDC) technique, which has been used for electrical characterizationof several dielectric materials, such as ionic crystals and polymers, for many years [8,9]. It has also been successfully applied also to semiconductor investigation in the 90 s [10,11], and it is still a successful technique nowadays [12,13]. TSDC refers to the field induced depolarization current upon buildup of charged defect centers in highly resistive semiconductor materials placed between two electrodes. Although this is a well known technique, it is described in some details in experimental section, below. This sort of experiment gives birth to depolarization current bands, which are related to dipole-like defects in the material, originally randomly oriented throughout the sample, which are polarized by an electric field applied at room temperature, and the sample is cooled down. The dipoles relax to thermodynamically

* Corresponding author.
E-mail address: luis.scalvi@unesp.br (L.V.A. Scalvi).

https://doi.org/10.1016/j.chemphys.2023.112004
Received 7 October 2022; Received in revised form 20 March 2023; Accepted 23 June 2023
Available online 25 June 2023
0301-0104/© 2023 Elsevier B.V. All rights reserved.

more stable configuration on temperature rise. The electric dipoles are assumed to be diluted throughout the sample so that the dipoles interactions can be disregarded, which means that the current generated by dipoles relaxation is proportional to the number of relaxing dipoles (a first order relaxation kinetics) [14]. The fitting of TSDC band by a Debye single curve or an asymmetric relaxation time distribution [15] yields important relaxation parameters such as activation energy, pre-exponential factor of the Arrhenius equation and relaxation time associated to defects [16–19].

It is interesting to mention that dipoles can be investigated by other more sophisticated techniques such as used for subatomic particles as electrons [20] and neutrons [21]. One may investigate the electron dipole moment by applying a strong electric field to a substance that has unpaired electron spin, at low temperature. The dipole interaction would lead to a net sample magnetization that can be detected with a superconducting quantum interference device (SQUID) magnetometer [22]. The dipole orientation measurements may also be performed by variation of photoluminescence (PL) exciton decay rate from time-resolved PL and optical analysis [23].

TSDC technique has been used on the characterization of La-doped $TlInS_2$ layered semiconductor (ferroelectric), and the short circuit current passing through the sample is relative to charged defects localized mainly close to the sample surface, besides its volume [12]. TSDC applied to polymer/molecular semiconductor all-organic composites, reveals that blending the semiconductor into a heat-resistant dielectric polymer brings extra carrier trap sites to the resultant all-organic composites [24].

In the $GaAs/SnO_2$ heterostructure there is many sort of defects, which may be charged due to the statistical distribution of free charges in the matrix and their energy level inside the bandgap. Considering the charged defects existing in the semiconductor layers, there are some possibilities for dipole formation. In the GaAs layer, the EL2 defect is responsible for a free electron concentration larger than the intrinsic concentration [25]. In order to accomplish this effect the EL2 must acquire a positive charge ($EL2^+$). The activation energy determined by thermally stimulated photocurrent measurements (TSPC) is about 0.26 eV of the midgap level EL2 in GaAs, which corresponds to lattice relaxation for changing between stable and metastable states [26]. Deep level transient spectroscopy (DLTS) data suggest that the EL2 level is a about 0.8 eV below the conduction band bottom and it has positive charge ($EL2^+$) [27].

In the SnO_2 side, the *n*-type behavior of this oxide semiconductor comes mainly from oxygen vacancies and interstitial tin atoms [28–30]. Oxygen vacancies can exist as neutral, singly or doubly charged vacancies, where singly ionized acts as shallowdonors and the doubly ionized as deep donors [29], even though there are many conflicting reports on the shallow or deep level nature of their related electronic states [30]. In the present paper, the existing dipoles were modeled by considering that oxygen vacancies present a single positive charge (V_O^+), because the doubly ionized vacancies does not change the idea presented here, only the value of the respective activation energies. The rare-earth ion (Er) presents oxidation state 3+, which means that when substituting Sn^{4+} it needs to capture an electron to stabilize, assuming an acceptor behavior [31,32]. Electrons are abundant in SnO_2 and then, the Er atom captures one electron and acquires negative charge (Er^-).

The relevance of studying vacancies is present even in indoor/outdoor environmental monitoring and specific disease diagnosis, related to the development of ultra-sensitive gas sensors, where V_O is considered to be crucial on gas sensing characteristic [26,33,34], as well as they play crucial roles in the temperature dependence of the photoluminescence [35].

In this paper, the possible formation of dipoles in the heterostructure system $GaAs/SnO_2$, where the top layer (tin dioxide) is doped with Er, is investigated, by the thermally stimulated depolarization current (TSDC) technique. Specific features related to bias orientation and the presence of stray (room) lights are observed and associated with the dipole formation.

2. Experimental section

2.1. Heterostructure sample deposition

Tin dioxide (SnO_2) solution production was carried out by using $ErCl_3$ added to SnO_2solution to form SnO_2:1at%Er^{3+}. This solution was dried and the obtained powder is used as precursor material in the resistive evaporation procedure [6]. The deposition was carried out placing the powder in a molybdenum crucible as the evaporation vessel. The residual pressure in the chamber was about 10^{-5} torr.The deposited samples were thermally annealed at 500 °C.

The GaAs substrates are from Wafer World and have semi-insulating property (not intentionally doped) with the face oriented in the plane (1 0 0) and the flat (cross section of the substrate) oriented in the plane (1 1 0). They have a thickness of 500–600 μm with both sides polished.

The sample was completed by deposition of metallic In contacts to extreme of both materials, by the use of shadow masks, again by using the resistive evaporation technique. The sample final configuration is shown in Fig. 1.

2.2. Optical and structural characterization data

Optical transmittance measurements were performed using a Perkin Elmer spectrophometer, model Lambda 1050 Uv/Vis/Nir, in the range 1800–250 nm (scanning in the direction of increasing energy). With the transmittance data, the optical bandgap of SnO_2 and GaAs were evaluated using the Tauc plot [36]. It was considered direct bandgap transition for GaAs and indirect for SnO_2, then squared optical absorption coefficient (α^2) and the square root ($\alpha^{1/2}$), respectively, were plotted as function of the energy of the incident light.

X-ray diffraction measurements were carried out on a MiniFlex 600/RIGAKU using Cu radiation (Kα = 1.5405 Å) and Ni filter to attenuate the Kβ radiation. The scan was performed at a rate of 2°/min, in the range 20 to 80° in the powder mode.

2.3. Thermally depolarization current (TSDC) procedure

To carry out TSDC measurements, a Janis cryostat has been used, where the sample is kept under pressure of 10^{-6} torr. The polarizing voltage is in the range −20 V to +20 V, and the TSDC technique is accomplished as follows: the electric field is applied for 5 min and the temperature is decreased to 77 K (liquid nitrogen temperature). When this temperature is reached, the electric field is removed and the temperatureis raised at fixed rate. During the temperature rise, the depolarization current is measured and recorded, using the same electrodes used for sample polarization. A 6517A Keithley electrometer is used to apply the voltage as well as to measure the current through the electrodes. The heating rate is 5 K/min and the sample temperature ismeasured through a sensor placed directly on the sample holder.

Electrical characterization of the heterostrucure was also accomplished through current as function of the applied voltage, and current

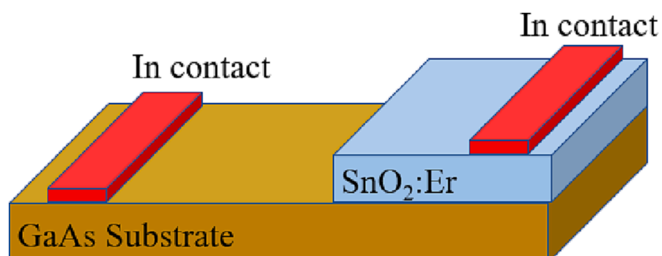

Fig. 1. Sample final configuration for TSDC measurement.

as function of temperature, for fixed bias. The biasing and collecting of electrical current was performed with the aid of Keithley electrometers models 6517 and 6517A.

3. Results and discussion

3.1. Optical and structural characterization

The heterostructure has individually the expected optical absorption edges for SnO_2 and GaAs. Fig. 2 shows the optical transmittance of SnO_2 and GaAs, and the bandgap evaluated according to the Tauc plot [36]. The inset in Fig. 1 shows the heterojunction expected from the junction of monolayers of these two semiconductor materials, with the respective bandgaps and the interface barrier, which may act as rectifying barrier for applied voltage parallel to the growth direction (through the interface barrier).

Considering the existing charged defects in the semiconductor layers, as already mentioned, there are some possibilities of charged defects that may contribute in the dipole formation. In the GaAs layer the EL2 defect, which becomes positively charged ($EL2^+$) after releasing electrons, and, in the SnO_2 side, the *n*-type behavior of this oxide semiconductor comes mainly from oxygen vacancies and interstitial thin atoms [28–30], which presents positive charge (represented by V_O^+ in the present work) due to ionization, and Er acceptor, which becomes negative after trapping one electron (Er^-).

X-ray diffraction patterns of SnO_2 powder doped with 1at% Er^{3+}, used for preparing the heterostructure sample, is presented in Fig. 3. The analysis of Fig. 3 shows that the diffractogram present the typical planes of SnO_2 crystals with rutile structure (JPCD 2003 file 01-088-0287). The inset in Fig. 3 shows diffractogram for the GaAs substrate, with the peaks being associated with the structure zincblend (JCPDS 2003 00-032-0389). The very definite and narrow peaks related to planes (2 0 0) and (4 0 0), confirm the singlecrystalline nature of the GaAs layer. More X-ray diffraction data may be found at Supplementary Information file (fig. S1) as well as SEM for the heterostructure GaAs/SnO_2 (fig. S2).

3.2. TSDC data

In the TSDC procedure, previous to any sample polarization, charged defects are randomly distributed throughout the respective layers, since there is, at this moment, no external factor, such as an electric field. Thus, these defects are as sketched in Fig. 4, with formed dipoles randomly distributed.

For the TSDC procedure, the temperature lowering rate is 10 K/min.

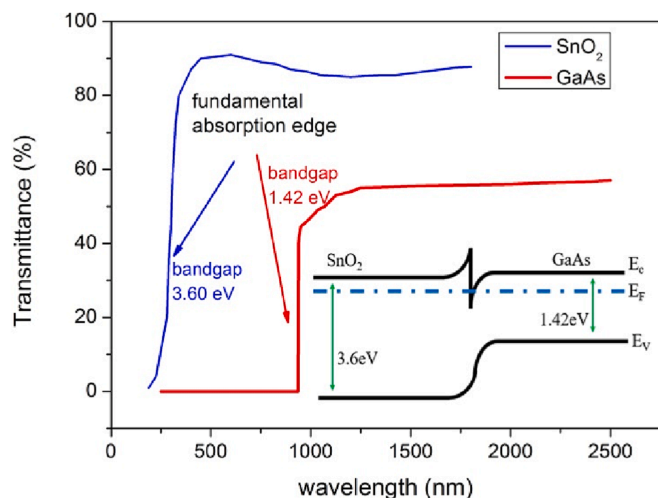

Fig. 2. Transmittance as function of incident light energy wavelength for GaAs and SnO_2:Er. Inset: heterojunction of these two semiconductors.

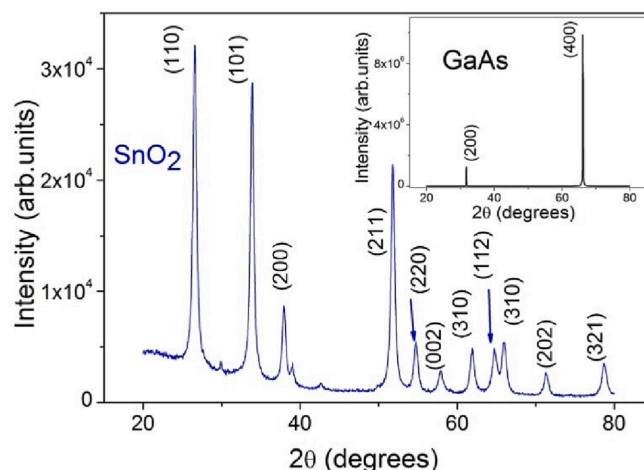

Fig. 3. XRD data for SnO_2:1at%Er powder, used in the resistive evaporation. Inset: XRD for semi-insulating GaAs substrate.

Before starting the temperature rise ramp, there is a waiting time for discharge (tdc) of about 20 min for a possible sample capacitive discharge to occur. In the application of the electric field, one terminal of the sample is in the GaAs layer and another in the SnO_2 top layer.

The measurements plotted in Fig. 5 were performed with the polarization starting at 300 K (room temperature) and remaining with the electrical voltage (Vp) applied to the sample throughout the cooling process, from 300 K to 80 K. Fig. 5 represents a comparison of TSDC current measurements for three values of positive polarization voltages: +20 V, +15 V and +10 V, and two values of negative polarization voltage: −20 V and −15 V. These values of tension where chosen based in results for standard mineral samples [18] and considering the electrical conductivity and the sample thickness, to the electric field does not damage the sample. The positive bias (also call here as forward) means that the GaAs layer is positive, where the opposite (reverse bias) is when the GaAs is negatively polarized. Concerning the positive bias, a band with an absolute peak at −271 pA is observed for polarization of + 20 V, and a reduction of approximately 20% in the maximum (peak) value of the current is observed for Vp = +15 V. In the case of polarization voltage Vp = +10 V, was performed keeping the other measurement parameters unchanged and it was verified that, differently from what occurred in the reduction from +20 V to +15 V, in the reduction from +15 V to +10 V there was no decrease in the maximum value of electrical current measured at a temperature of 260 K, remaining at –217 pA, both for Vp = +15 V and for Vp = +10 V. A more noticeable difference can be observed in the range from 270 K to 330 K, where there are three clear oscillations (smaller bands) in the current values at 285 K, 305 K and 310 K for the Vp = +20 V and +15 V which are smaller when the electric field voltage value was +10 V, that is, for the lower voltage. The three TSDC bands apparently tend towards the formation of a single broad band.

In order to verify influence of the direction of the applied electric field on the shape of the TSDC curve, negative polarization was performed, which are also seen in Fig. 5. The cooling rate was 10 K/min per minute, with a capacitive discharge time of 20 min at 80 K. The temperature rise ramp was 5 K/min. In the black curve, the sample was polarized with Vp of +20 V and in the red curve, the polarization was −20 V, keeping the other measurement parameters (cooling and heating rate, pressure, dark condition) unchanged. It is possible to observe that there is not a symmetrical behavior with regard to the magnitude of the electric current as a function of the temperature obtained during the controlled temperature rise. For the +20 V polarization, as already mentioned, a peak at −271 pA occurs, at a temperature of 260 K, which takes place after the current values have become smaller and positive during heating from 80 K to 245 K, with current values between 0 and 50

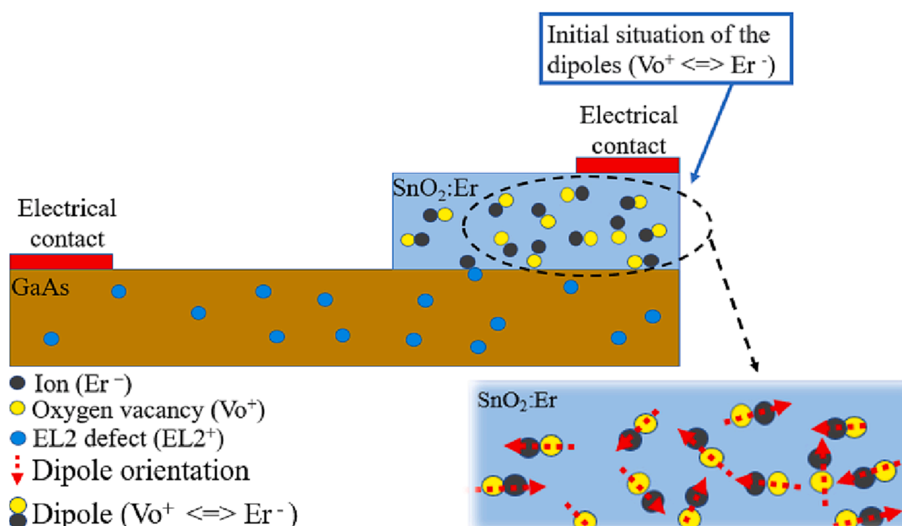

Fig. 4. Initial arrangement of the constituent charged particles of the GaAs/SnO_2:Er heterostructure, before applying any electrical bias or temperature variation. The inset represents an enlarged part, showing the randomly distribution of dipoles in the SnO_2 side of the sample.

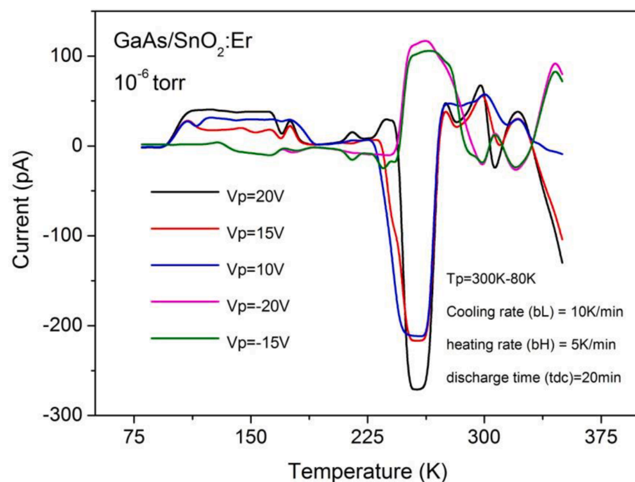

Fig. 5. TSDC measurements for polarized GaAs/SnO_2 heterostructure sample in the temperature range of 300 K to 80 K, under pressure of 10^{-6} torr, in the dark, with polarization voltage (Vp) of 10 V, 15 V, 20 V, –15 V and −20 V, with final temperature of 350 K.

pA, with a small variation (small peaks) at 170 K and 225 K, of with current values of −38 pA and −11 pA, respectively. The largest current variation occurs between temperatures of 240 K and 270 K, with the maximum at 255 K and 260 K. Between 270 K and 330 K, it is seen again positive and more stable current values, with a wider band between 270 K and 305 K, with two sharper peaks of -40 pA at 280 K and −121 pA at 305 K. After that, another higher current value is recorded, − 40pA at 320 K, and from there, the current goes into decline with a tendency to negative values at 335 K up to 350 K. On the other hand, for the polarization of –20 V, the TSDC current remains practically constant between 80 K and 245 K, with slightly negative values, but very close to zero, with a slight variation at 215 K, but much smaller absolute value than the black curve (+20 V). In this case, there is also a peak in the current after 245 K, with its highest value being 118 pA at 260 K. It is possible to verify that in this measurement, the current return to levels prior to the temperature of 245 K is slower, that is, the peak is wider, and it is not possible to see in this measurement the large variation that occurred at 275 K as in the measurement with positive bias. Oscillations (smaller bands) that occur between 300 K and 350 K for +20 V, also occur for −20 V, but with inverted signals and visibly lower intensity.

Taking the positive 20 V bias as a reference (peak of –271 pA), there is a difference in the absolute value of 56% lower for negative bias. This sample behavior for different forms of polarization gives us an indication of how the possible dipoles, formed preferentially by V_O^+, $EL2^+$ and Er^- interact with each other in the SnO_2 material structure and at the GaAs/SnO_2 interface, when they are subjected to external factors: actuation of an electric field and controlled temperature variation. The absence of some peaks with negative polarization implies that some types of dipoles can be polarized by the positive voltage, but have negligible polarization in the reverse bias, which can be related to the relaxation of defects, in some cases, with difficulty in moving the position of equilibrium, to form the polarized dipole.

Concerning the negative bias of –15 V, the controlled heating curve is quite similar to the curve with Vp = -20 V, that is, the same sort of difference observed for the positive polarization voltages of +15 V and +20 V was not verified. The curves (red and blue) have practically the same current values over the entire temperature range, 80 K to 350 K, with slightly higher values on the Vp = −20 V curve between 250 K and 265 K.. There is also a slight ripple in current at 215 K and 235 K on the Vp = −15 V curve, which does not happen with Vp = −20 V.

The influence of polarization on the dipoles behavior with different applied voltages may also be analyzed through the area under the curve of each measurement and the width at half maximum of each curve. This is presented in Table 1. These two parameters are directly related to the amount of charge that moves during the TSDC procedure, as well as the amount of oriented dipoles/cm^3. It is possible to observe that the area under the curve is greater for Vp = +20 V, reducing slightly when Vp = +15 V, even though the width at half maximum has increased, whereas there is no significant change between Vp of +15 V and +10 V. On the other hand, when the polarization is reversed (-20 V and −15 V), the values of the area under the curve are much smaller compared to the

Table 1
Parameters obtained from TSDC bands with distinct bias (Vp).

Vp (V)	Imax (pA)	Temperature (K)	Width at half maximum (K)	Area under TSDC curve (arb. units)
20	−271	255	21	392
15	−217	260	24	391
10	−211	260	28	422
−15	104	265	33	229
−20	118	265	34	301

measurements with direct polarization. However, the same effect is not observed for the width at half maximum of these measurements, which shows, once again, the different ways that the dipoles behave for each bias direction, as well as their different relaxation times, because although some curves have smaller areas (−20 V and −15 V), their width at half maximum is larger, which suggests, a higher "slowness" for the dipoles to return to their equilibrium positions, which means that Er^-, $EL2^+$ and Vo^+ dipoles must interact with the electric field and temperature differently for each type of bias, in good agreement with the asymmetry of the relaxing dipoles.

Fig. 6 shows measurements performed on the sample without the cryostat window shut, to verify the difference related to measurements carried out with the sample completely in the dark. Measurements for polarizations 20 and −20 V are reproduced for comparison, plus a measurement where there was no polarization on temperature cooling. In the case of the TSDC measurement performed without any type of electric field application, it is possible to observe that the current values are practically unchanged during the entire temperature rise process, that is, basically there is no occurrence of electric current bands. There is only a slight increase in the values after the temperature of 250 K, from 5 pA to 40 pA at the temperature of 325 K, remaining at values close to this value until 350 K. On the other hand, in the measurements where polarization is accomplished, the application +20 V and –20 V during the temperature decrease from 300 K to 80 K, under room light, an increase in the current values during the temperature rise is observed. The initial behavior was similar to the measurements in the dark, but there was noformation of a TSDC band, as the values remained almost constant from 80 K to 235 K, when there was sharp increase in the current value, for both +20 V and –20 V polarization. When Vp was –20 V, the TSDC current increased from 235 K until reaching a maximum value of 210 pA at 320 K, whereas for Vp +20 V, the maximum value is –290 pA at 325 K. It is worth mentioning that for the case of the measurement of Vp –20 V there was also a small oscillation of the current observed between 220 K and 235 K. Clearly, light has a significant influence on the dipoles formation and relaxationin the GaAs/SnO_2:Er heterostructure, leading to distinct behavior in the dark or in the presence of room light, even though this light has low ultraviolet radiation (that would responsible for bandgap transition in the SnO_2 layer).

The influence of light is clearly observable in Fig. 6, both for +20 V and −20 V. The total charge Q released by the depolarization process is proportional to the volumetric dipole density (dipoles/cm^3) [37,38]. It causes some perturbation in the polarized dipoles, which are, initially, metastably and statistically oriented by the electric field. If ϕ is the average value of the dipole inclination angle, measured in the direction of application of the electric field (may be determined through a Boltzmann distribution [37]), when the dipoles are randomly oriented throughout the sample, ϕ is about 90°, which means that the dipoles are in thermal equilibrium. The electric field rotates these dipoles, bringing them to a higher energy position, which is maintained by polarization. The temperature decrease freezes these dipoles with $\phi = 0$ and the temperature increase provides enough energy to the dipoles to overcome the activation barrier and return to their original position, randomly distributed throughout the sample.

For the case of the measurement carried out under room lights, the irradiation supplies additional energy, concomitant with the increase in temperature, not allowing the completion of the dipole relaxation process, which would promote a decrease in current (movement of charges to original positions), instead, these superimposed effects, show the result seen in the two curves with light of Fig. 6, i.e. the current gradually increases until it stabilizes around −300 pA for forward polarization and around 200 pA for reverse polarization, both around 310 K, a point at which the combination of light and temperature probably no longer promote significant changes in the behavior of the dipoles.

The influence of light on the TSDC results in natural materials [39,40], such as amethyst, is closely related to the existing defects in this sort of sample, since it presents interstitial or substitutional defects of iron ions (Fe^{3+} or Fe^{4+}) that are responsible for the decrease in TSDC peak values when the measurement was carried out under the influence of an Ar^+ laser (lines 488 nm or 541 nm) compared to the measurement without the incidence of laser on the sample. As iron atoms are responsible for the formation of color centers of amethyst, as this material has optical absorption at wavelengths very close to those of Ar^+ laser, the decrease or destruction of these TSDC bands is associated with iron dipoles in the structure [39]. On the other hand, in the GaAs/SnO_2 heterostructure, although measurements with light influence were not performed with monochromatic light, it is very likely that room light radiation also acts as a factor of modification of TSDC bands, as seen in Fig. 6, mainly in the GaAs layer since ambient light has energy larger than the bandgap of this semiconductor. The reduction or destruction of the TSDC bands associated with the Er^-, $EL2^+$ or V_O^+ dipoles by light radiation is linked to an additional component, influencing the dipole relaxation time and having enough optical activation energy to modify the dipoles, in addition to the already known thermal effect, caused by the controlled increase in temperature.

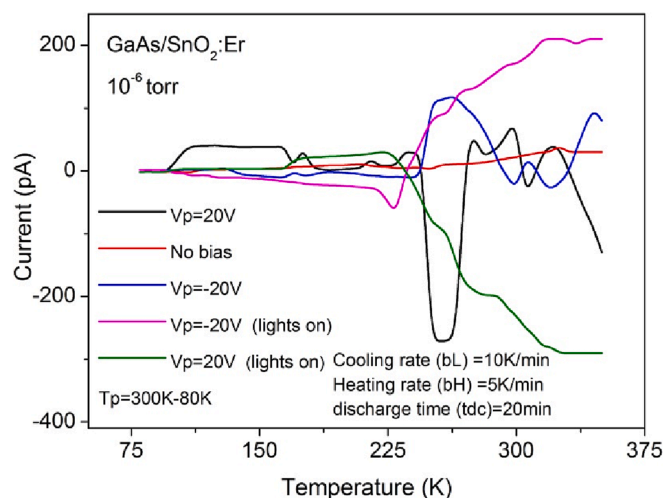

Fig. 6. TSDC measurements for heterostructure GaAs/SnO_2:Er biased in the range 300 K to 80 K, under a pressure 0f 10^{-6} torr, in the dark and under influence of stray light, with polarization of −20 V and +20 V. Curves obtained in the dark are shown for comparison.

3.3. Current –voltage characteristics of the interface

Fig. 7(a) represents a curve of current versus temperature curve for a fixed applied voltage of 10 V, where the applied voltage and the current data colleting are taken simultaneously. The detail in Fig. 7(a) is an Arrhenius plot to obtain the activation energy of the ionized level near room temperature. Fig 7(b) is a current-voltage curve at several temperatures, in the dark, which shows a diode-like behavior. The superior inset is a magnification of the measurement at 200 K, in order to exhibit a better visualization. The inferior inset is the sample diagram and the setup of the measurement. The effect of ambient light can be seen in Fig. 7(a) where the current is measured at a fixed voltage of 10 V, and ambient light is allowed to enter the sample at a certain temperature. It is important to note that in the case of this figure, it is not a TSDC measurement, where the voltage source is removed to collecting the current data, that is, in this case the voltage source and electrometer are connected to the same terminals, as can be seen in the detail of Fig. 7(b), which is a schematic diagram of the sample for these measurements, with the electrometer placed in series with the voltage source and the GaAs/SnO_2 sample.The value for the activation energy obtained is 847 meV, which is rather high, but could be associated with EL2 level, intrabandgap defect in GaAs [27]. However, it is better associated with the interfacial potential barrier. Wang and Ledge [41] obtained a value

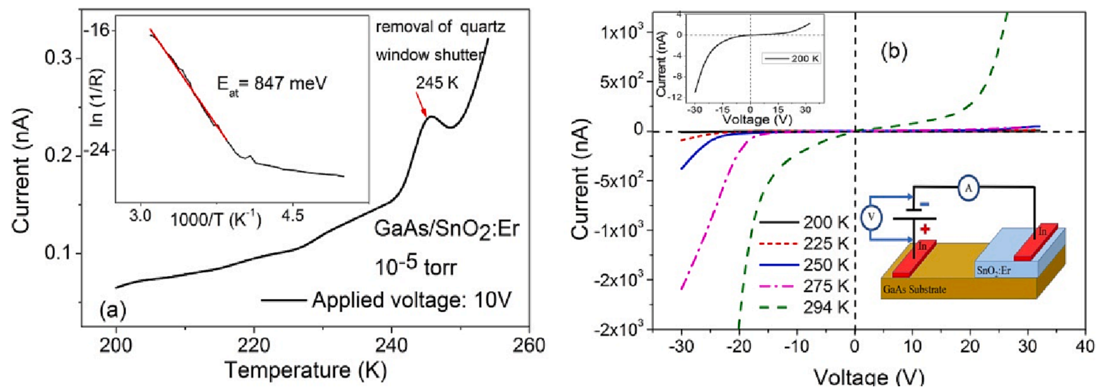

Fig. 7. (a) Current as function of temperature for fixed applied bias of 10 V. Inset: Arrhenius plot to obtain activation energy close to room temperature (b) current – voltage at several temperatures. Superior inset: current – voltage at 200 K. Inferior inset: sample diagram and measurement setup.

in the order of 0.4 V for the threshold voltage in an *n-n* GaAs/SnO_2 diode (translated to energy means 400 meV). Importantly, they observed that incident light radically changes the current–voltage characteristics of the diode curve. The I-V characteristics of Fig. 7(b) show the asymmetry of electrical transport through the interface potential barrier and the temperature dependence. Considering that the rectifying behavior is associated with the positive I-V, which means the GaAs layer with positive bias, it is clear that the electrical transport is more difficult in the direction from GaAs to SnO_2 layer, whereas the transport from SnO_2 to GaAs layer takes place after some threshold voltage, with is practically zero at room temperature (294 K) and increases when temperature decreases. This is quite consistent with the shape of the band structure diagram of the device as sketched in the inset of Fig. 2, which shows asymmetry due to band bending at interface. Moreover, it is also consistent with a picture of interface dipoles leading to TSDC bands, which display asymmetry depending on the polarization direction as seen in Figs. 5 and 6.

3.4. Dipole identification

Fig. 8(top) schematizes the dipole behavior in this heterostructure, whereas Fig. 8(bottom) shows the interface situation in detail. The GaAs layer is positively biased, whereas the SnO_2 layer is negatively biased, at 300 K. This applied voltage orients the dipoles in a predominant direction, and, as the temperature drops to 80 K, they are “frozen” in this position. The most probable contributions for this configuration is: 1) orientation of dipoles formed by V_O^+ and Er^- in SnO_2, with the positive charge upwards, according to the geometry of the sample; 2) tendency to form dipoles Er- and $EL2^+$ at the interface of these materials. However, in the latter case, the relative position of these ions is a obstacle to a perfect alignment with this sort of applied electric field, since the $EL2^+$ is located in the GaAs, which is the bottom layer, and the tendency of the field would be to take it up, while that Er^- would be displaced downwards by the action of the electric field, but it is located in the SnO_2 layer. Another hypothesis is the formation of dipoles in the interfacial region of SnO_2 with V_O^+ and the excess of electrons in the GaAs layer, but the electric field would tend to displace these electrons away from the interface, leaving the formation of this dipole unfeasible. On the other hand, if the polarization were reversed, that is, with SnO_2 positively polarized, this condition is favored, as will be discussed in detail below. Looking at Fig. 5, it is observed that for inverted polarization, the main TSDC bands are wider, which may indicate that there is an overlap of two bands, one connected to the dipoles in SnO_2 side and the other that would be the interface contribution. The higher value and thinner current band for polarization with +20 V can be related to the greater contribution of the relaxation of the charged defects with the alignment of the dipoles in which the defect of positive charge is shifted upwards.

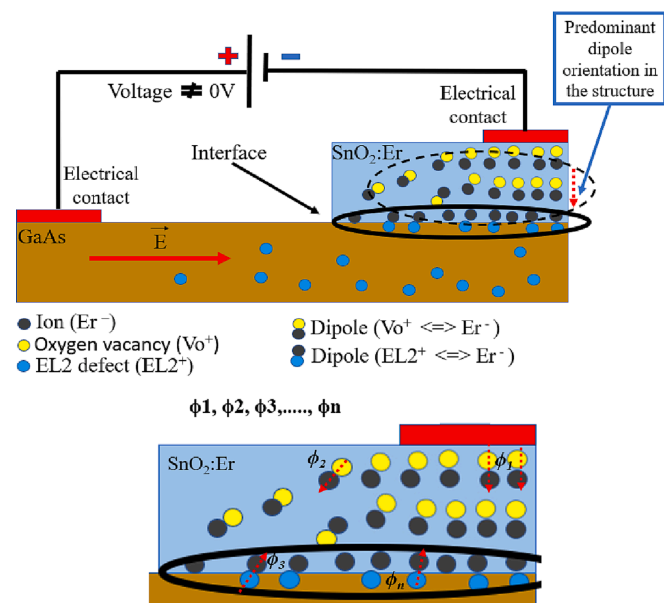

Fig. 8. (top) Diagram of dipoles orientated by electric field action at room temperature.**(bottom)** Distribution of dipole angles related to the applied electric direction.

Observing the diagram of Fig. 8, one can verify the proposed dipole orientation hypothesis, due to the fact that the electric field favors a certain direction for the dipoles present in the SnO_2 layer of the heterostructure, according to the dominant orientation direction. For these components of the dipole orientation, the tendency is that this orientation is, according to the electric field, so that the negative charges move as much as possible in the opposite direction of the electrical contact of the SnO_2 layer, consequently, the positive ones tend to be directed, forcing an approach to electrical contact. On the other hand, those dipoles formed in the interface region tend to have a different orientation, as shown in the circled detail of the interface in Fig. 8 (top), and shown in detail in Fig. 8 (bottom). The same electric field causes the highest concentration of Er^- (negative) ions at the interface, which are not in dipole formation with SnO_2 oxygen vacancies, but may tend to align with the positively charged EL2 defects of the GaAs interface. As already mentioned, the relative position of these ions is an obstacle to a perfect alignment with this sort of applied electric field, since the $EL2^+$ is located in the GaAs, while Er^- is in the SnO_2 layer. This latter situation leads to an increase in the average angle value of the formed dipoles.

The formation of a certain number of dipoles/cm^3 according to these two possibilities leads to a certain concentration of dipoles in the whole heterostructure, ***N***, with each dipole of magnitude ***p***, is subjected to an electric field ***E***, and has potential energy ***U*** per dipole:

$$U = -pE = -pE\cos\varphi \quad (1)$$

where **cos *ϕ*** represents the average value of the angle between the dipole and the applied electric field direction, which in general follows a Boltzmann distribution [19,40]. As the current density or the total polarization charge depends on the total polarization of the system (which depends on the number of dipoles oriented by the electric field) and on the activation energy (*Ea*) for defect reorientation within the host material, the more these dipoles are aligned with the direction in which the electric field acts, the greater the measured current will be in the depolarization process, since the total polarization of the system is:

$$P = Np\cos\varphi \quad (2)$$

Fig. 9 shows the connection of the electrometer, which replaces the voltage source, using the same terminals. It is used to record the electrical current in the heating process of the sample, back to room temperature at fixed rate (5 K/min). During the temperature rise, the dipoles, previously polarized by the electrical at cooling down process, return to their equilibrium positions, randomly distributed throughout the sample. The dipole charge movement originates the TSDC band recorded, as also shown schematically in Fig. 9, and corresponding to a faced down band (negative current), since a polarization where the voltage source is connected with the GaAs layer positively biased, originates a negative current.

The area delimited by the TSDC curve is the depolarization current, which is proportional to the number of dipoles of a given type present in the sample. The area under the current curve allows us to calculate the total polarization charge (*Q*). In this case, the ions move from one equilibrium position to another, that is, they move between two potential wells, by acquiring enough thermal energy to overcome this potential barrier [39]. In the present case, as there is large amount of concentrated dipoles, there will be a great displacement of charges during the heating process.

The TSDC current is also related to the potential barrier needed to be overcome by the dipoles during the ion relaxation, allowing the randomly disorientation in the rise of temperature. The relaxation frequency for the dipole disorientation *α(T)* follows an Arrhenius behavior [13]:

$$\alpha(T) = \exp(-\frac{Ea}{k_BT}) \quad (3)$$

where k_B is the Boltzmann constant, and Ea is the activation energy for dipole disorientation at temperatureT, as defined previously. The current density *j(T)*, generated by the decay in polarization for a constant rate heating process b_H, in a TSDC experiment is given by:

$$j(T) = P_0\alpha_0\exp(-\frac{Ea}{k_BT})\exp[-\frac{1}{b_H}\int_{tdc}^{t}\alpha(T)dt] \quad (4)$$

Here, α_0 is the characteristic relaxation frequency (t→∞), P_0 is the initial equilibrium polarization, *tdc* is the discharge time, which means the time to start the temperature rise with current data collecting. Considering that the temperature is raised linearly with time, the heating rate b_H (=dT/dt) is constant. The peak temperature, T_p, for the current peak can be obtained by differentiating Eq. (4), and after a few simplifications, the activation energy can be obtained approximately by [13]:

$$Ea = k_BT_p\ln(\frac{T_p^2}{b_H}) \quad (5)$$

Using the data in Fig. 5, the main TSDC peak may be plotted as function of the applied voltage, as shown in Fig. 10,which allows visualizing more clearly the difference between the TSDC peaks obtained for positive and negative polarizations. In the blue curve, the actual values of the measured peak currents are shown, including the current signal in the Electrometer reading. The analysis of this curve shows that the TSDC peaks were distributed within a current range between 118 pA and −271 pA (right y axis). On the other hand, the black curve of Fig. 10 allows us to compare between the maximum absolute values of each current peak (left y axis), according to the applied polarization. This analysis shows that we have a 57% difference in the TSDC peak values for the polarization voltages at which the highest peaks are obtained, ie. +20 V and −20 V. During the sample heating process, that is, in the same stage of dipole relaxation provided by the TSDC technique, it is very clear that the behavior of the dipoles formed by the EL2, Er defects or oxygen vacancies (V_O) is distinct and dependent on the polarity of the electric fieldsource, otherwise, the curves would display symmetrical TSDC peaks in the positive and negative portions of the electric current axis as a function of the temperature of Fig. 5.

According to equation (5), all the observed TSDC peaks for the several polarization valuesyieldthe calculated activation energies. Ea plotted as function of peak temperature yields a linear format, since the b_H is constant in this paper and as the TSDC peak temperature increases, the activation energy obtained by equation (5) increases linearly. On the other hand, the obtained activation energy may be plotted as function of the TSDC peak current, which is shown in Fig. 11.

In Fig. 11, the most evident peaks correspond to activation energies of 213 meV for forward bias, where the influence of the positive polarization magnitude is clearly identified. On the other hand, for negative polarization no influence of the bias magnitude is verified.

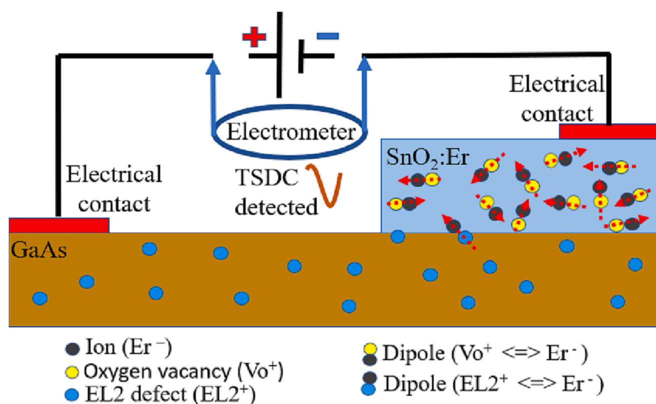

Fig. 9. Diagram representing the origin of current, recorded as function of temperature rise, with the electrometer connected and the dipole thermally induced reorganization to equilibrium states.

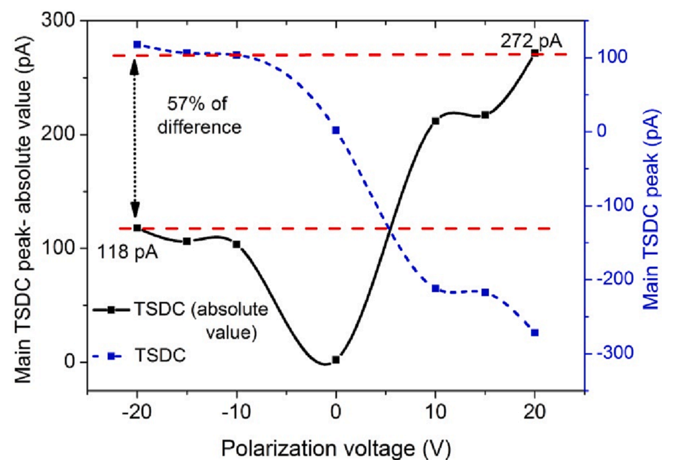

Fig. 10. Main TSDC peak as function of applied bias voltage. The y axis in the left side is the absolute value (module) whereas in the right side is the actual value.

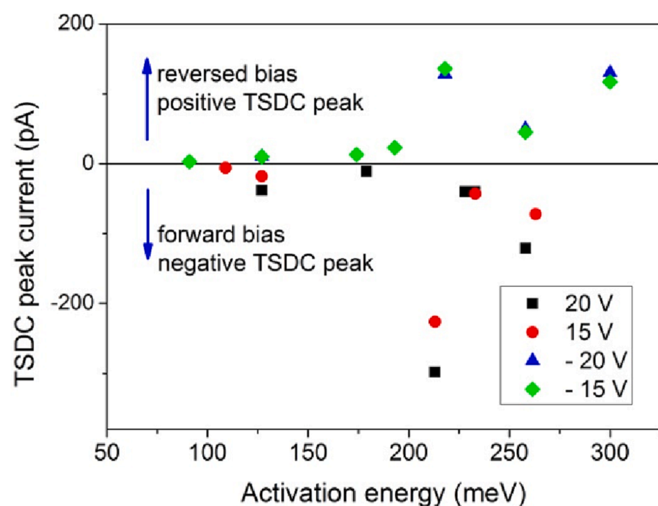

Fig. 11. TSDC peak as function of evaluated activation energy for several polarization voltages in the GaAs/SnO_2:Er heterostructure. Forward bias means the GaAs is positively biased and reverse when it is negative.

The activation energy determined by thermally stimulated photocurrent measurements(TSPC)is about 0.26 eV for the energy barrier from an optically excited metastable EL2* state to the ground state ($EL2^o$) of the defect in GaAs [26], whereas when deep level transient spectroscopy (DLTS) is used it is found about 0.8 eV below the conduction band [27]. TSPC energy barrier is related to a lattice relaxation around the defect.The proximity between the activation energy valuesdetermined by TSPC and by TSDC in this work is a strong indication that at least one of the TSDC peaks the GaAs/SnO_2:Er heterostructure may be related to the process of polarization and subsequent relaxation of dipoles that have the EL2 defect as one of their constituents, since we have activation energy values of 0.213 eV, 0.228 eV, 0.233 eV and 0.258 eV, as can be seen in Fig. 11. Moreover, the dipole current involves also a lattice relaxation, which may explain the closeness between energies measured by TSPC and TSDC. It is also worth mentioning that, even for other polarization voltages (-20 V, +15 V and −15 V), the most significant TSDC peaks are those obtained at temperatures where the activation energy is in the range 0.2 eV and 0.3 eV, also clearly observed in the Fig. 11.

In addition to the EL2 defect, oxygen vacancies (Vo^+) and Erbium ions (Er^-) are very relevant in this structure. Studies have shown activation energy values of oxygen vacancies, between 0.15 eV and 0.30 eV below the conduction band minimum [30,35], The acceptor level of Er in SnO_2 is about 0.1 eV above the valence band top [42], The activation energy forEr ions in SnO_2 nanocrystals is 25 meV, comparable tothe binding exciton energy for SnO_2 [43],while for Erbium films the activation energy varies between 0.128 eV and 0.817 eV, depending on the grain size [44]. Some of the activation energies observed in the Fig. 11 are in the range of 0.1 eV, but no such low temperature band was verified to lead to 25 meV of activation energy, which suggest that in the TSDC bands recorded in Fig. 5, the activation energies are related to oxygen vacancies and Er acceptor level in the SnO_2 side, but the crystallite size may have influenced the obtained energies. Moreover, the largest peaks for positive bias, with 213 meV of Eat, with a current peak of −298 pA, and 218 meV with 128 pA for negative bias, has its bands destroyed by the stray light, whose rise to a permanently higher current starts just before the peak in the dark observed for measurements in the dark. It may correspond to the second ionization level of oxygen vacancies in SnO_2 [45], and maybe excited by the room lights and do not return to the original orientation.

All the calculated values of Ea, plotted in Fig. 11 are much smaller than the value calculated from the Arrhenius plot of Fig. 7 from current × temperature data (847 meV), which shows the distinct process of dipole reorientation and sample polarization through the heterostructure interface.

Fig. 12 represents the situation when the layers polarization is reverted, with GaAs layer negatively biased whereas the SnO_2 layer gets positive potential. It corresponds to the results of −15 V and −20 V in Fig. 4, where the TSDC current bands are positive.The action of the electric field in this case creates a tendency for the positive charges (in this case V_O^+) in the SnO_2 layer to move away from the contact region, and the negative ions (Er^-) to align upwards. Furthermore, it creates conditions for the V_O^+ ions from the SnO_2 interface region to attract free electrons from the GaAs layer, where they present greater mobility, to the same interfacial region. Then, the dipoles in this case are a little different from the forward polarization case. The higher value of current for polarization with +20 V is probably related to the higher concentration of different types of dipoles, or to the activation barrier between the polarized and random states. For the voltage of −20 V, it is possible to verify a lower value of the main TSDC peak, approximately 57% smaller than the current peak for the −20 V polarization, as shown in Fig. 10. As can be seen in Fig. 12, by inverting the positive and negative poles of the voltage source, consequently the direction of the electric field within the GaAa/SnO_2:Er heterostructure, the relative positions of the positive and negative charges within each layer of the heterostructure is changed, and distinct possibilities for dipole formation are observed in each case. The TSDC curves of Fig. 5 are certainly related to the amount of dipoles/cm^3, formed by positive and negative charges oriented by the electric field during the TSDC process. With the negative pole of the voltage source connected to the SnO_2:Er layer, there is a higher concentration of oriented dipoles formed by localized ions in the structure, which results in a higher current value for the polarization voltage of +20 V. In addition, the total charge density reorganizes during a classic process of dipole relaxation by thermal activation.

The picture representing the TSDC band recorded during temperature rise, for the reversed polarization voltage is similar to Fig. 9, with the difference that it represents a positive TSDC band, and corresponds to a smaller amount of dipoles reorienting, mainly at the interface, which justifies the lower value of main TSDC band in this case.

4. Conclusion

The application of the TSDC technique to the heterostructure system GaAs/SnO_2 has yield interesting bands whose magnitude depends on the polarization direction, being more prominent when the GaAs side is the positive electrode. The possible formation of dipoles suggests the participation of well known defects in these semiconductor layers, such as the EL2 defect in the GaAs side, whereas oxygen vacancies and Er ions seems to play fundamental role in the SnO_2 layer. The dipole relaxation activation energies are found in the range 0.2 eV to 0.3 eV, in good agreement with typical ionization energies reported for these defects. The main TSDC bands are modified by stray (room) light, since the obtained dipole relaxation energies may correspond to the ionization second ionization level of oxygen vacancies in SnO_2, which may be excited by the room lights, eliminating the extra electron, and avoiding the dipole return to the original orientation.

Temperature dependent current-voltage (I-V) characteristics of this heterostructure show the asymmetry of electrical transport through the interface potential barrier. A rectifying behavior is observed when the GaAs layer is positively biased, which suggests a more difficult electrical transport from GaAs to SnO_2 layer, whereas the transport from SnO_2 to GaAs layer takes place after some threshold voltage, which increases when temperature decreases. This is quite consistent with the shape of the band structure diagram of the device, which shows asymmetry due to band bending at interface.

The present investigation aims to contribute to the understanding of electrical properties of these semiconductor compounds, and the possible relationship with luminescence properties coming from the detected defects. We believe that such a comprehension may be crucial

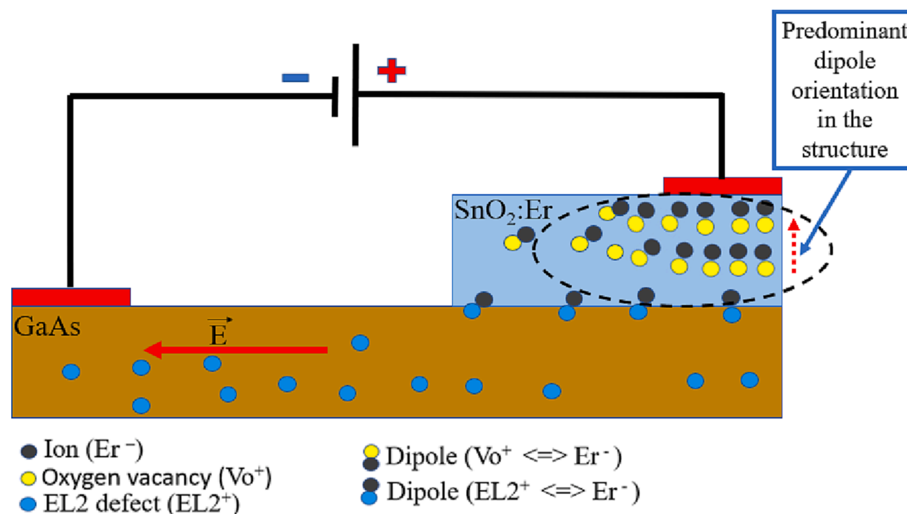

Fig. 12. Dipole orientation in the GaAs/SnO_2:Er heterostructure for negative bias of the GaAs substrate, showing a lower concentration of dipoles at the interface region.

in the design and operation of optoelectronic devices, based on the heterostructure GaAs/SnO_2.

CRediT authorship contribution statement

Fabricio T. Russo: Conceptualization, Data curation, Formal analysis, Investigation, Writing – original draft. **Diego H.O. Machado:** Supervision, Validation, Visualization. **Luis V.A. Scalvi:** Methodology, Supervision, Writing – review & editing.

Declaration of Competing Interest

The authors declare that they have no known competing financial interests or personal relationships that could have appeared to influence the work reported in this paper.

Data availability

Data will be made available on request.

Acknowledgements

Authors acknowledge Prof. Jose H. Silva for the GaAs substrates and Prof. Fenelon M. Pontes for using the XRD equipment. FAPESP (Proc. 2016/12216-6 and 2021/08853-9), and CNPq for financial support.

Appendix A. Supplementary data

Supplementary data to this article can be found online at https://doi.org/10.1016/j.chemphys.2023.112004.

References

[1] T.F. Pineiz, L.V.A. Scalvi, M.J. Saeki, E.A. Morais, Interface Formation and Electrical Transport in SnO_2:Eu^{3+}/GaAs Heterojunction Deposited by Sol-Gel Dip-Coating and Resistive Evaporation, J. Electron. Mater. 39 (2010) 1170–1176. https://link.springer.com/article/10.1007/s11664-010-1161-0.

[2] T.F. Pineiz, E.A. Morais, L.V.A. Scalvi, C.F. Bueno, Interface formation of nanostructured heterojunction SnO2: Eu /GaAs and electronic transport properties, Appl. Surf. Sci. 267 (2013) 200–205, https://doi.org/10.1016/j.apsusc.2012.10.097.

[3] C.F. Bueno, L.V.A. Scalvi, M. Siu Li, M.J. Saeki, Luminescence of Eu3+ in the thin film heterojunction GaAs/SnO_2, Opt. Mater. Express 59 (2015) 61–71, https://doi.org/10.1364/OME.5.000059.

[4] D.H.O. Machado, L.V.A. Scalvi, A. Tabata, J.H.D. Silva, Interface conduction and photo-induced electrical transport in the heterojunction formed by GaAs and Ce^{3+}-doped SnO_2, J. Mater. Sci.: Mater. Electron. 28 (2017) 5415–5424. https://link.springer.com/article/10.1007/s10854-016-6202-x.

[5] C.F. Bueno, A.Y. Ramos, A. Bailly, E. Mossang, L.V.A. Scalvi, X-ray absorption spectroscopy and Eu^{3+}-emission characteristics in GaAs/SnO_2 heterostructure, SN Appl. Sci. 2 (2020) 1579. https://link.springer.com/article/10.1007/s42452-020-03344-3.

[6] D.H.O. Machado, J.H.D. Silva, A. Tabata, L.V.A. Scalvi, Influence of thermal annealing on the properties of evaporated Er-doped SnO2, Mater. Res. Bull. 120 (2019), https://doi.org/10.1016/j.materresbull.2019.110585.

[7] Y. Wang, J. Ma, F. Ji, X. Yu, H. Ma, Structural and photoluminescence characters of SnO_2: Sb films deposited by RF magnetron sputtering, J. Lum. 114 (2005) 71–76, https://doi.org/10.1016/j.jlumin.2004.12.003.

[8] G.F.L. Ferreira, M.T. Figueiredo, S.N. Fedosov, J.A. Giacometti, Thermally stimulated polarization in dye doped polystyrene explained via the Williams-Watts a–b relaxation model, J. Phys. D Appl. Phys. 31 (1998) 2051, https://doi.org/10.1088/0022-3727/31/16/015.

[9] R.C. Walker, H. Hamedi, W.H. Woodward, M. Lanagan, Thermally stimulated depolarization current spectra of cross-linked polyethylene and the influence of cross-linking byproducts, J. Pol. Sci. 58 (2020) 3142–3152, https://doi.org/10.1002/pol.20200470.

[10] L.V.A. Scalvi, L. Oliveira, E. Minami, M. Siu Li, Dipole relaxation current in n-type $Al_xGa_{1-x}As$, Appl. Phys. Lett. 63 (1993) 2658-2660, https://doi.org/10.1063/1.110795.

[11] L.V.A. Scalvi, L. Oliveira, M. Siu Li, Light-induced relaxing dipoles in n-type $Al_xGa_{1-x}As$, Phys. Rev. B 51 (1995) 13864–13867, https://doi.org/10.1103/PhysRevB.51.13864.

[12] M.H.Y. Seyidov, R.A. Suleymanov, F.A. Mikailzade, E.O. Kargın, A.P. Odrinsky, Characterization of deep level defects and thermally stimulated depolarization phenomena in La-doped $TlInS_2$ layered semiconductor, J. Appl. Phys. 117 (2015), 224104, https://doi.org/10.1063/1.4922347.

[13] B. Wang, D. Look, K. Leedy, Deep level defects in β-Ga_2O_3 pulsed laserdeposited thin films and Czochralski-grown bulk single crystals by thermally stimulated techniques, J. Appl. Phys. 125 (2019), 105103, https://doi.org/10.1063/1.5049820.

[14] C. Bucci, R. Fieschi, G. Guidi, Ionic thermocurrents in dielectrics, Phys. Rev. 148 (1966) 816–823, https://doi.org/10.1103/PhysRev.148.816.

[15] S. Havriliak, S. Negami, A complex plane representation of dielectric and mechanical relaxation processes in some polymers, Polymer 8 (1967) 161–210, https://doi.org/10.1016/0032-3861(67)90021-3.

[16] R. Chen, Y. Kirst, Analysis of thermally stimulated processes, first ed., Pergamon Press, New York, 1981.

[17] J. Prakash, Role of the Background Current in Analysing the ITC Spectrum, Physica Status Solidi A 98 (1986) 247–252, https://doi.org/10.1002/pssa.2210980128.

[18] R.M.F. Scalvi, M.S. Li, L.O. Ruggiero, L.V.A. Scalvi, Light-Induced Electric Dipole relaxation in synthetic and natural alexandrite, Radiat Eff. Defects Solids 156 (2001) 295–299, https://doi.org/10.1080/10420150108216908.

[19] P.R. Prezas, B.M.G. Melo, L.C. Costa, M.A. Valente, M.C. Lança, J.M.G. Ventura, L.F.V. Pinto, M.P.F. Graça, TSDC and impedance spectroscopy measurements on hydroxyapatite, β-tricalcium phosphate and hydroxyapatite / β-tricalcium phosphate biphasic bioceramics, Appl. Surf. Sci. 424 (2017) 28–38, https://doi.org/10.1016/j.apsusc.2017.02.225.

[20] W. Bernreuther, M. Suzuki, The electric dipole moment of the electron, Rev. Modern Phys. 63 (1991) 313–340, https://doi.org/10.1103/RevModPhys.63.313.

[21] C. Abel, S. Afach, N.J. Ayres, et al., Measurement of the Permanent Electric Dipole Moment of the Neutron, Phys. Rev. Lett. 124 (2020), 081803, https://doi.org/10.1103/PhysRevLett.124.081803.

[22] S.K. Lamoreaux, Solid-state systems for the electron electric dipole moment and other fundamental measurementsPhys, Rev. A 66 (2002), 022109, https://doi.org/10.1103/PhysRevA.66.022109.
[23] I.J. Ko, H. Lee, J.H. Park, G.W. Kim, R. Lampande, R. Podeb, J.H. Kwon, Anaccurate measurement of the dipole orientation in various organic semiconductor films using photoluminescence exciton decay analysis, Phys. Chem. Chem. Phys. 21 (2019) 7083, https://doi.org/10.1039/C9CP00965E.
[24] C. Yuan, Y. Zhou, Y. Zhu, J. Liang, S. Wang, S. Peng, Y. Li, S. Cheng, M. Yang, J. Hu, B. Zhang, R. Zeng, J. H, Q. Li, Polymer/molecular semiconductor all-organic composites for high-temperature dielectric energy storage, Nat. Commun. 11 (2020) 3919, https://doi.org/10.1038/s41467-020-17760-x.
[25] J.C. Bourgoin, T. Neffati, The energy level of the EL2 defect in GaAs, Solid State Electron. 43 (1999) 153–158, https://doi.org/10.1016/S0038-1101(98)00199-3.
[26] Y.N. Mohapatra, V. Kumar, Determination of activation energy for thermal regeneration of EL2 from its metastablestate by thermally stimulated photocurrent measurements, J. Appl. Phys. 64 (1998) 956, https://doi.org/10.1063/1.341906.
[27] H.J. von Bardeleben, D. Stievenardand, D. Deresmes, A. Huber, J.C. Bourgoin, Identificationof a defect in a semiconductor: EL2 in GaAs, Phys. Rev. B 34 (1986) 10–15, https://doi.org/10.1103/PhysRevB.34.7192.
[28] P.A. Agoston, K. Albe, R.M. Nieminen, M.J. Puska, Intrinsic *n*-Type Behavior in Transparent Conducting Oxides: A Comparative Hybrid-Functional Study of In_2O_3, SnO_2, and ZnO, Phys. Rev. Lett. 103 (2009), 245501, https://doi.org/10.1103/PhysRevLett.103.245501.
[29] S. Mehraj, M.S. Ansari, A.A. Al-Ghamdi, Alimuddin, Annealing dependent oxygen vacancies in SnO_2 nanoparticles: Structural, electrical and their ferromagnetic behavior, Mater. Chem. Phys. 171 (2016) 109–118, https://doi.org/10.1016/j.matchemphys.2015.12.006.
[30] J. Buckeridge, C.R.A. Catlow, M.R. Farrow, A.J. Logsdail, D.O. Scanlon, T.W. Keal, P. Sherwood, S.M. Woodley, A.A. Sokol, A. Walsh, Deep vs shallow nature of oxygen vacancies and consequent *n*-type carrier concentrations intransparent conducting oxides, Phys. Rev. Mater. 2 (2018), 054604, https://doi.org/10.1103/PhysRevMaterials.2.054604.
[31] E.A. Morais, L.V.A. Scalvi, S.J.L. Ribeiro, V. Geraldo, Poole-Frenkel effect in Er doped SnO2 thin films deposited by sol-gel-dip-coating, Phys. Status Solid A 202 (2005) 301–308, https://doi.org/10.1002/pssa.200406919.
[32] E.A. Morais, L.V.A. Scalvi, Decay of photo-excited conductivity of Er-doped SnO_2 thin films, J. Mater. Sci. 45 (2007) 2216–2221, https://doi.org/10.1007/s10853-006-1320-0.
[33] L. Wang, S. Ma, X. Xu, J. Li, T. Yang, P. Cao, P. Yun, S. Wang, T. Han, Oxygen vacancy-based Tb-doped SnO_2 nanotubes as anultra-sensitive sensor for ethanol detection, Sens. Actuators B 344 (2021), 130111, https://doi.org/10.1016/j.snb.2021.130111.
[34] H. Sawadaand, K. Kawakami, Electronic structure of oxygen vacancy in Ta_2O_5, J. App. Phys. 86 (1999) 956, https://doi.org/10.1063/1.370831.
[35] E. Choi, D. Lee, H.-J. Shin, N. Kim, L. De Los S. Valladares, J. Seo, Role of Oxygen Vacancy Sites on the Temperature-Dependent Photoluminescence of SnO_2 Nanowires, J. Phys. Chem. C 125 (2021) 14974−14978. https://doi.org/10.1021/acs.jpcc.1c02937.
[36] J. Tauc, Optical properties and electronic structure of amorphous Ge and Si, Mater. Res. Bull. 3 (1968) 37–46, https://doi.org/10.1016/0025-5408(68)90023-8.
[37] A.N. Papathanassion, I. Sakellis, J. Grammatikalis, S. Sakkopoulos, E. Vitoratos, E. Dalas, An insight into the localization of charge carriers in conducting polyaniline by analyzing thermally stimulated depolarization signals, Solid State Commun. 125 (2003) 95–98, https://doi.org/10.1016/S0038-1098(02)00707-X.
[38] R.M. Neagu, E.r. Neagu, The distribution of the relaxation times and the thermally stimulated depolarization currents, J. Optoelectronics Adv. Mater. 8 (2006) 949–955. https://old.joam.inoe.ro/arhiva/pdf8_3/3Neagu1.pdf.
[39] F.T. Russo, R.M.F. Scalvi, L.V.A. Scalvi, M.V.G. Vismara, Photo-Induced Dipole Relaxation Current in Natural Amethyst, Mater. Res. 15 (2012) 461–466, https://doi.org/10.1590/S1516-14392012005000052.
[40] S.U. Cortezão, W.M. Pontuschka, M.S.F. Da Rocha, A.R. Blak, Depolarizationcurrents (TSDC) and paramagnetic resonance (EPR) of iron in amethyst, J. Phys. Chem. Solids 64 (2003) 1151–1155, https://doi.org/10.1016/S0022-3697(03)00043-X.
[41] E.Y. Wang, R.N. Ledge, General properties of SnO_2-GaAs and SnO_2-Ge Heterojunction Voltage Cells, IEEE Trans. Electron Dev. 25 (1978) 800–803, https://doi.org/10.1109/T-ED.1978.19173.
[42] J. Ren K. Li, J. Shen, C. Sheng, Y. Huang, Q. Zhang. Effects of rare-earth erbium doping on the electrical performance of tin-oxide thin film transistors, J. Alloys Compounds 791 (2019) 11-18, https://doi.org/10.1016/j.jallcom.2019.03.277.
[43] J. del-Castillo, V.D. Rodrıguez, A.C. Yanes, J. Méndez-Ramos, Energy transfer from the host to Er3+ dopantsin semiconductor SnO_2 nanocrystals segregatedin sol–gel silica glasses, J. Nanopart. Res. 10 (2008) 499–506. https://link.springer.com/article/10.1007/s11051-007-9283-x.
[44] H. Savaloni, M.A. Player, Influence of deposition conditions and of substrate on the structure of uhv deposited erbium films, Vacuum 46 (1995) 167–179, https://doi.org/10.1016/0042-207X(94)E0033-U.
[45] S. Samson, C.G. Fonstad, Defect structure and electronic donor levels instannic oxide crystal, J. Appl. Phys. 44 (2003) 4618–4621, https://doi.org/10.1063/1.1662011.